Towards a model for the dissociative recombination of the CO^{2+} dication: states and couplings

N. Vinci[1], N. de Ruette[2], F. O. Waffeu Tamo[3,4], O. Motapon[4], M. Fifirig[5], O. Crumeyrolle[3], X. Urbain[2], J. Tennyson[1] and I. F. Schneider[3]

[1] Department of Physics and Astronomy, University College London, Gower St., London WC1E 6BT, UK

[2] Department of Physics, Université Catholique de Louvain, Louvain-la-Neuve, Belgium

[3] Laboratoire de Mécanique, Physique et Géosciences, Université du Havre, 25, rue Philippe Lebon, P.O. Box 540, 76058 Le Havre Cedex, France

[4] Center for Atomic, Molecular Physics and Quantum Optics, University of Douala, Avenue de la Liberté - AKWA, BP 8580, 00237 Douala Littoral, Cameroon

[5] Department of Physics, Faculty of Chemistry, University of Bucharest, Bd. Regina Elisabeta 4-12, Bucharest, RO-70346, Romania

Abstract.

Preliminary results which will be used for calculations of dissociative recombination (DR) of electrons with the CO^{2+} dication are presented. The measurements of CO^{2+} dissociative recombination rates, the first for any multiply charged target, were obtained at the ASTRID heavy ion storage ring. The present study starts from the potential energy curves for the first 7 electronic states of CO^{2+} and results for low-energy e^- – CO^{2+} scattering that were obtained in recent *R*-matrix calculations (Vinci and Tennyson, J Phys. B, 37 (2004) 2011). Meanwhile, in order to apply an MQDT-type approach that has been previously used for NO^+, we concentrate on partial the resonance series converging to the $^1\Delta$ target state in the CO^+ $^2\Sigma^+$ symmetry. The quasi-discrete vibrational spectrum of the CO^{2+} ground electronic state is explored.

1. Introduction

Small molecules with more than a single charge are inherently unstable due to Coulomb forces. However it is well established that some dications can live for significant length of time. CO^{2+} is a prime example of such a dication and one may well be of astrophysical importance.

Dissociative recombination (DR) provides a possible destruction route for the long-lived metastable states of dications. CO^{2+} was the first multiply charged target to have its DR rate measured. These measurements were performed at the ASTRID storage ring [1] and were subsequently repeated using a corrected calibration formula for the absolute scale of rate coefficients [2]. Recently the DR rate has been re-measured using the TSR storage ring [3], confirming the re-calibrated dissociative recombination rate measured previously [2].

Our aim is to study the DR of CO^{2+} by combining resonance curves and widths computed with the R-matrix method [5,6] with a Multichannel Quantum Defect Theory (MQDT) approach [7] to the treatment of the nuclear dynamics. Such an approach was used successfully by two of us to study the DR of NO^+ [4]. Here we present our progress on this project.

The present work follows a detailed theoretical analysis devoted mainly to the resonant CO^+ states and their autoionization widths [6]. This analysis, based on *R*-matrix calculations, showed that seven CO^{2+} states provide the cores of these resonances, and contribute in a coherent way to the autoionization. However, binary interactions between a Rydberg state pertaining to one CO^{2+} core (e.g. X $^3\Pi$) and a Rydberg state pertaining to another CO^{2+} core (e.g. $^1\Delta$) cannot be evaluated from the resonance width computed in Ref. [6] by a deconvolution procedure.

Therefore, in order to investigate the dissociative recombination dynamics, the R-matrix calculations had to be partly re-launched in order to provide to the MQDT computational procedure [4, 7] with these "channel to channel", or "2-channel" interactions. Mores specifically, for every pair of ionic cores, we have to perform separate "2-channel", rather than "7-channel" calculations. Preliminary data, relevant to the DR rates, are presented here. These data arise from the CO^+ $^2\Sigma^+$ resonance series converging to the $^1\Delta$ target state only. The choice of these states is based on their favorable crossings with the CO^{2+} ground state curve. Low-lying mono-excited $^2\Sigma^+$ CO^+ Rydberg states ('bound states'), relevant to resonant contributions to DR through the 'indirect process', are also considered.

2. Molecular Data

The lowest dissociative limit in figure 1 from Ref. [6], C^+ (^2P_u) + O^+ (^4S_u), is 35.986 eV above the $X^1\Sigma^+$ state of CO [8,9]. Our energy of the X $^3\Pi$ state of CO^{2+} at equilibrium bondlength is -111.4871 E_h as calculated using Natural Orbitals (NOs) and a complete active space configuration interaction representation; see Table 1 in [5]. In the above

cited figure, this minimum is fixed to the experimental value [10] in eV. Figure 1 details the $^3\Pi$ and $^1\Delta$ target states dissociation limits as well as the DR atomic limits. Inclusion of the scattering electron leads to resonance series such as those displayed in figure 2. These have been calculated using both the 7-channel target close-coupling expansion used previously and a reduced 2-channel model. It should be noted that figure 2 corrects the energy scale of figure 5 in the work of Vinci and Tennyson [6], for which the unit label was not correct.

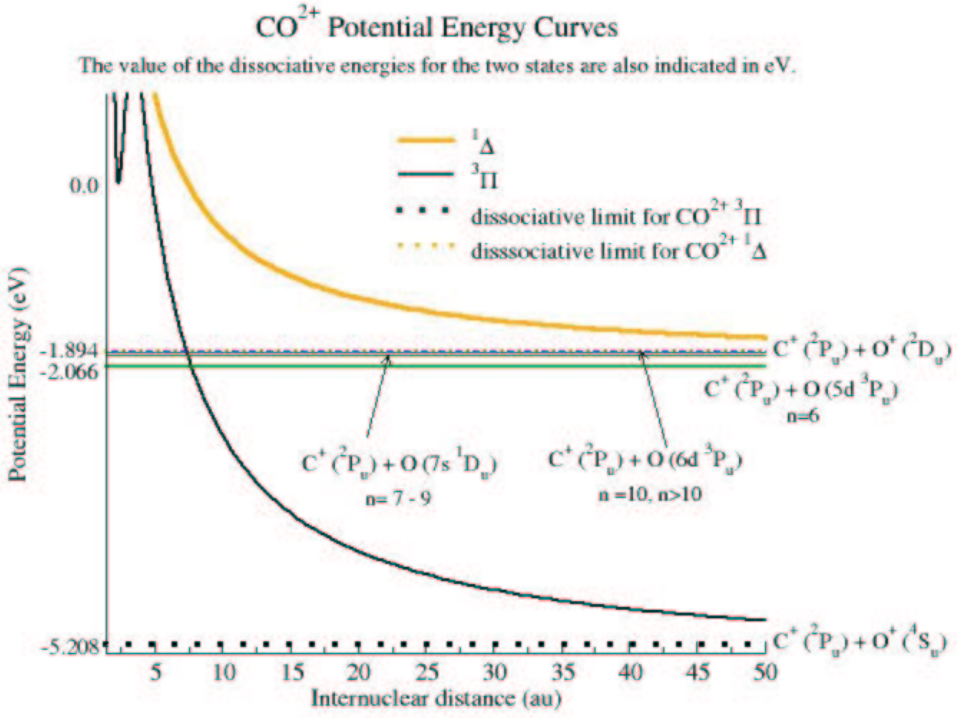

Figure 1. The atomic dissociative limits of the $^3\Pi$ and $^1\Delta$ states of CO^{2+} are compared with the DR atomic limits that are associated to the n^{th} resonances series in the continuum of CO^+.

3. CO^{2+} ground state vibrational dynamics

To accurately model the CO^{2+} DR, one needs electronic energy potential curves for CO^{2+} and CO^+ over a broad range of internuclear distances. Therefore, we extended the CO^{2+} data available from Vinci and Tennyson [6] using those obtained recently by Eland *et al* [11]. Figures 1 and 3 show that the $^3\Pi$ CO^{2+} electronic energy curve displays, as do some of those corresponding to excited states, a barrier at intermediate internuclear distance. This barrier allows the potential to support vibrational states with finite lifetimes with respect to the auto-dissociation. Calculations of the vibrational energy

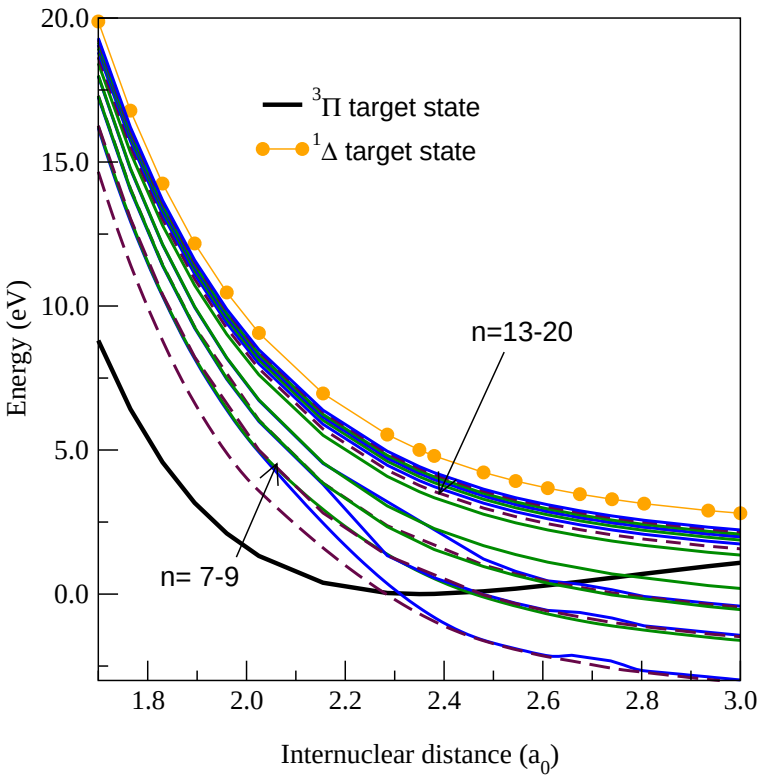

Figure 2. Resonance positions for the $^2\Sigma^+$ total symmetry for the series converging to the CO^{2+} $^1\Delta$ state. Full curves represent 7- channel calculations and dashed curves 2- channel ones.

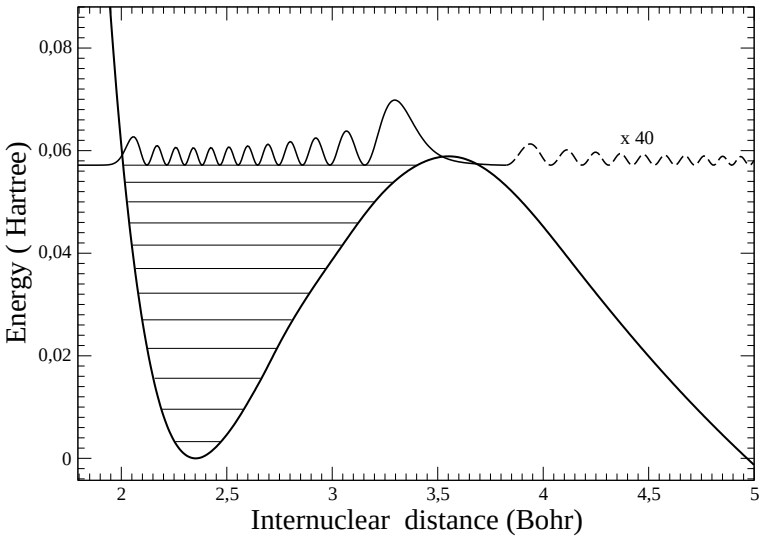

Figure 3. The vibrational levels of CO^{2+} in its $^3\Pi$ ground electronic state. The vibrational probability density for the highest vibrational level ($v = 11$) is represented, after multiplication by 40 in the classical forbidden region.

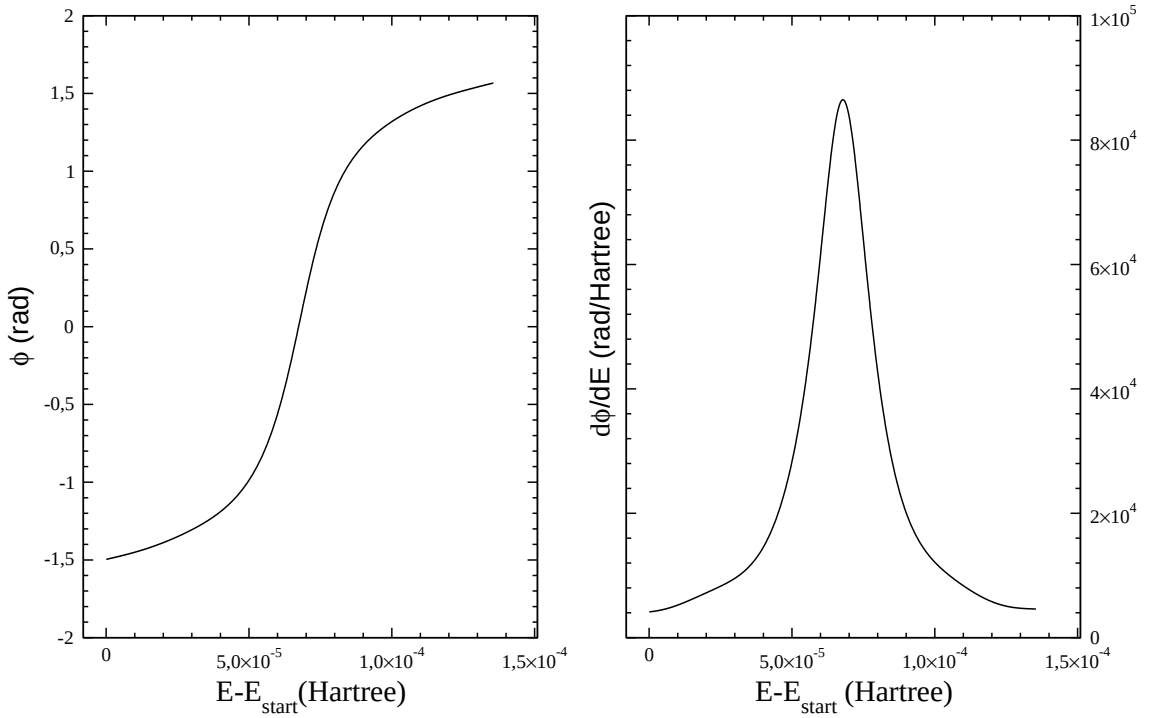

Figure 4. Detection of the quasi-discrete vibrational levels of CO^{2+} electronic ground state, illustrated for $v = 11$. The sudden variation of the phaseshift of the vibrational wavefunction in the asymptotic region (left) results in a Lorentzian profile for its derivative (right), from which the width is deduced. E_{start} (close to the vibrational level to be determined) is the minimum value of the energy range where the exploration is performed

.

levels and of their lifetimes for the CO^{2+} ground state have been performed using a method previously elaborated and tested on the CO^{+} ion [12]. It relies on the accurate detection of the sudden phase-shift variation characterising the wave-functions χ_N of the resonant states in the asymptotic region [13-16]. This behaviour is described essentially by the formulae:

$$\chi_N(R) = \kappa R\left[j_N(\kappa R) + \tan\phi_N \ \cdot n_N(\kappa R)\right], R > R_a \tag{1}$$

$$\kappa = \sqrt{2\mu(E - V_{as})/\hbar^2} \tag{2}$$

$$\phi_N(E) = \arctan\left[\frac{\kappa j'_N(\kappa R_a) - \gamma_N j_N(\kappa R_a)}{\kappa n'_N(\kappa R_a) - \gamma_N n_N(\kappa R_a)}\right] \tag{3}$$

$$\gamma_N = \left.\frac{\chi'_N(R)}{\chi_N(R)}\right|_{R_a} \tag{4}$$

$$\phi^r_N = \phi^{(0)}_N + \arctan\frac{\Gamma}{2(E_r - E)} \tag{5}$$

$$\frac{d\phi^r_N}{dE} = \frac{\Gamma/2}{(E_r - E)^2 + (\Gamma/2)^2} \tag{6}$$

where R is the internuclear distance, E_r is the resonance (quasi-discrete state) energy, ϕ_N is the phase-shift – given for a certain rotational number N of the molecular system, μ is the reduced mass, V_{as} the asymptotic limit of the potential curve, R_a represents the lower limit of the asymptotic region (for which a reasonable value must be chosen), and j_N and n_N are spherical Bessel and Neumann functions respectively. The quasi-discrete vibrational states are characterised by the resonant behaviour of the phaseshift ϕ_N^r described by formula (5), corresponding to a Lorentzian form of the phaseshift's derivative as given by formula (6). $\phi_N^{(0)}$ represents the non-resonant, or background, part of the phaseshift in the region of the resonance, and the prime $'$ in formulae (3) and (4) stands for the derivative of the functions. Finally, Γ labels the resonance width, from which the lifetime

$$\tau = \frac{\hbar}{\Gamma} \tag{7}$$

is evaluated.

We shall restrict ourselves to rotationally cool dications, and consequently the rotational number N will be taken as 0.

The first step in detecting the resonant states is to solve the Schrödinger equation for an adjusted potential, where the barrier is absent. Once an approximate value for an energy level is determined, we can search for the true resonant energy exploring a limited range around this value. Figure 4 shows the behaviour of the phase-shift and of its derivative in the resonance region. The procedure is used to determine accurately quasi-discrete levels, their widths, see eq. (5), and their wave-functions, see Figure 3. The quasi-discrete states are characterised by a significant amplitude of the wave-function in the classical allowed region, and a very reduced one in the classically forbidden region, which is the opposite behaviour to the that found for "free" (continuum) vibrational states. As the energy of a quasibound state decreases so does its width and the determination of the resonance energy and width becomes numerically difficult. This means that the determination of these characteristics for the ground and the first excited states has not so far proved possible, red and it will have to wait for a calculation performed using quadruple-precision. Meanwhile, the energies and the wave-functions of these low-lying states are quite well described by an approximate calculation where the barrier is replaced by a flat potential.

The energy levels, widths and the corresponding lifetimes for v = 7, 8,...,11 are given in table 1. Also given are their approximate values evaluated within the semi-classical approximation of Gamow and improved by the quantum correction of Connor and Smith [14-16], as well as the values calculated in [11]. The differences between our data and those of Eland and co-workers come mainly from the different values of the $^3\Pi$ potential curve computed in ref. [6], with respect to those computed in ref. [11], at small internuclear distances. Another source of differences is the use of different numerical methods used in the two studies for solving the Schrödinger equation.

We notice that a complete caracterisation of the vibrational spectrum, including the highly excited vibrational states, is quite important for an accurate DR modelling.

v	7	8	9	10	11
$E^{(0)}$(a.u.)	0.0415733	0.0459022	0.0500139	0.0538235	0.0571639
E(a.u.)	***	0.0459023	0.0500141	0.0538236	0.0571596
Γ_{Gamow}(a.u.)	7.146E−19	3.794E−15	1.007E−11	1.088E−08	4.170E−06
Γ_{Connor}(a.u.)	7.189E−19	4.001E−15	1.050E−11	1.107E−08	4.157E−06
Γ(a.u.)	***	3.777E−15	9.807E−12	1.090E−08	3.680E−06
Γ_{Eland}(a.u.)	2.892E−19	2.628E−15	9.651E−12	1.401E−08	6.820E−06
τ_{Gamow}(s)	33.848	6.374E−03	2.401E−06	2.222E−09	5.800E−12
τ_{Connor}(s)	33.647	6.044E−03	2.303E−06	2.184E−09	5.812E−12
τ(s)	***	6.403E−03	2.466E−06	2.218E−09	6.572E−12
τ_{Eland}(s)	83.647	9.200E−03	2.506E−06	1.726E−09	3.546E−12

Table 1. Vibrational levels: exact energy E and approximate $E^{(0)}$ and corresponding widths Γ and lifetimes $\tau = \frac{\hbar}{\Gamma}$. "Gamow" and "Connor" stand for the semi-classical value and for that including the quantum correction respectively, whereas "Eland" stands for the values calculated in [11] which are given for comparison. "***" denotes quantum results absence due to numerical limitations. Scientific notation is used to denote powers of ten.

Indeed, although these latter states are involved mainly in the closed ionization channels, their contribution may play an important role in the DR cross-section, due to the channel-mixing effects [17].

The characterisation of the resonant ("quasi-discrete") states will serve as starting point for CO^{2+} dissociative recombination calculations. On the other hand, the lifetime evaluations can be used in applications related to "volcanic states" as support in energy storage, as previously invoked for the case of the He^{2+} dication [18].

4. Preliminaries for dissociative recombination dynamics and conclusions

Detailed calculations studying the DR dynamics are planned to be performed in Le Havre. These calculations are complicated by the sheer number of curves which have to be considered to model the DR in the system, even at very low electron impact energies. Besides the many curves in the $^2\Sigma^+$ series of CO^+ dissociative states illustrated in figure 3, converging to the $^1\Delta$ CO^{2+} potential, 5 further CO^+ series, either of different symmetries, or converging to different CO^{2+} limits provide numerous effective dissociative channels. On the other hand, as shown in figure 1, the 3 lowest CO^{2+} curves are almost degenerate, providing 3 different target states as possible starting points for the DR reaction.

Furthermore, it is not straightforward to predict the form of all the potential curves and widths involved for internuclear distances beyond $R = 3$ a_0. This means that further electron scattering calculation may well be necessary.

In conclusion, we have characterised the curves involved in the low-energy

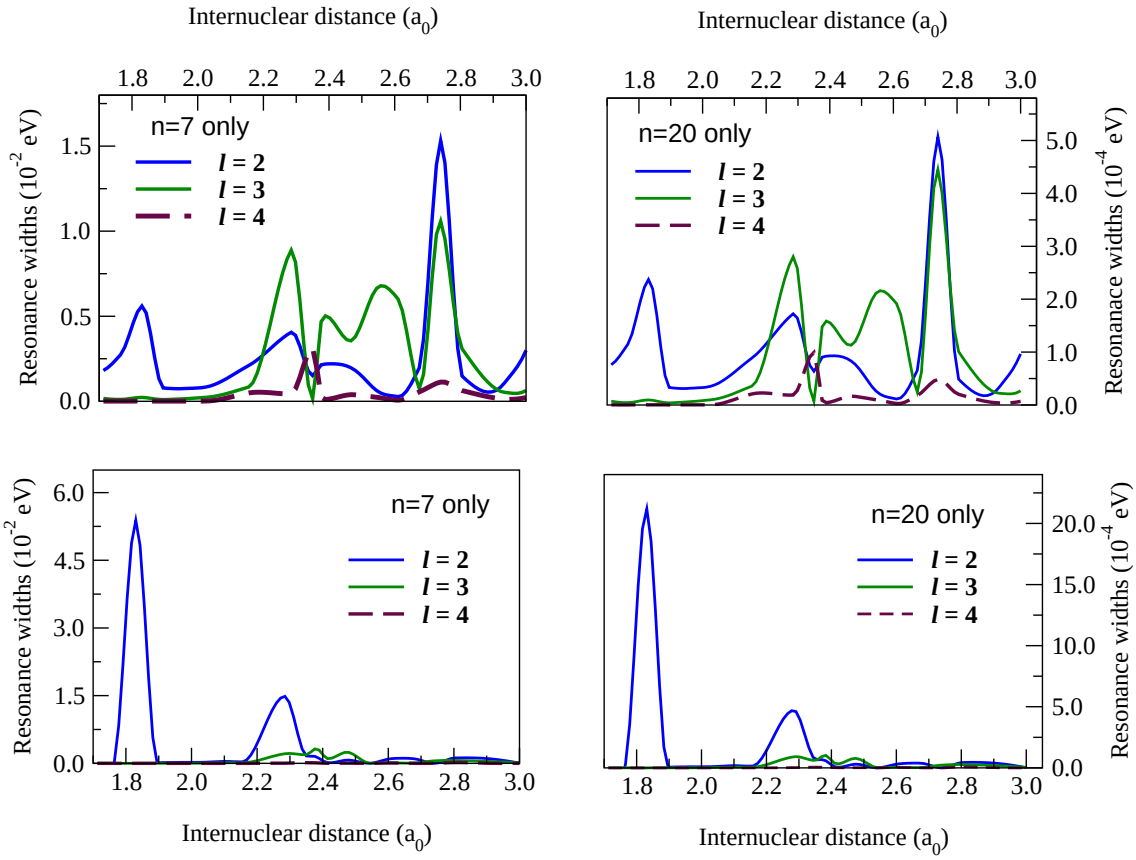

Figure 5. Resonance widths for the $^2\Sigma^+$ total symmetry for series converging to the CO^{2+} $^1\Delta$ state. Results are displayed for the series with $n = 7$ and $n = 20$ only and are obtained from two sets of calculations: the first one (top) is described in [6], and the second one (bottom) that retains only the two $^3\Pi$ and $^1\Delta$ target states in the close coupling expansion [6], see section 2.

dissociative recombination of CO^{2+} and started to study the nuclear dynamics of the problem. However, a complete model of the CO^{2+} DR will require a huge computational effort. So far, our studies have been restricted to the DR of the CO^{2+} ground state $^3\Pi$ into CO^+ $[^1\Delta(nd)]$ $^2\Sigma^+$ states. The coupling displayed in Figure 5, as well as the quantum defect characterising the Rydberg series of bound states of $^3\Pi$ core will be used in a preliminary partial evaluation of the cross section.

Further 2- channel calculations are currently being performed in order to provide all the DR-relevant energies and couplings, necessary for a complete quantitative description of the CO^{2+} DR process.

Acknowledgements

We thank Prof Annick Suzor-Weiner and Prof Helene Lefebvre-Brion for helpful discussions. This research was supported by a grant from the EU Electron Transfer Reactions research network, HPRN-CT-2000-00412.

References

[1]C. P. Safvan, M. J. Jensen, H. B. Pendersen, L. H. Andersen, Phys. Rev. A 60 (1999) R3361.
[2]K. Seiersen, O. Heber, M. J. Jensen, C. P. Safvan, L. H. Andersen, J. Chem. Phys. 119 (2003) 839.
[3]D. Zajfmann, private communication (2004).
[4]I. F. Schneider, I. Rabadán, L. Carata, J. Tennyson, L. H. Andersen, A. Suzor-Weiner, J. Phys. B: At. Mol. Opt. Phys. 33 (2000) 4849.
[5]L. A. Morgan, J. Tennyson C. J. Gillan, Computer Phys. Comms. 114 (1998) 120.
[6]N. Vinci, J. Tennyson, J. Phys. B: At. Mol. Phys. 37 (2004) 2011.
[7]A. Giusti-Suzor, J. Phys. B: At. Mol. Phys. 13 (1980) 3867.
[8]P. Lablanquie, J. Delwiche, M-J. Hubin-Franskin, I. Nenner, P. Morin, K. Ito, J. H. D. Eland, J-M. Robbe, G. Gandara, J. Fournier and P. G. Fournier, Phys. Rev. A 40 (1989) 5673.
[9]L. H. Andersen, J. H. Posthumus, O. Vahtras, H. Ågren, N. Eler, A. Nunez, A. Scrinzi, M. Natiello and M. Larsson, Phys. Rev. Lett. 71 (1993) 1812.
[10]G. Dawber, A. G. McConkey, L. Avaldi, M. A. MacDonald, G. C. King and R. I. Hall, J. Phys. B: At. Mol. Opt. Phys. 27 (1994) 2191.
[11]J. H. D. Eland, M. Hochlaf, G. C. King, P. S. Kreynin, R. J. LeRoy, I. R. McNab and J-M. Robbe, J. Phys. B: At. Mol. Opt. Phys. 37 (2004) 1.
[12]N. de Ruette, Diploma work, unpublished (2003).
[13]H. Abgrall, A. Giusti-Suzor and E Roueff,Astrophysical J.207 (1976) L69.
[14]B. H. Bransden and C. J. Joachain, "Physics of atoms and molecules", Printice Hall (2004).
[15]J. N. L. Connor, Mol. Phys.15 (1968) 621.
[16]J. N. L. Connor and A. D. Smith, Mol. Phys.45 (1982) 149.
[17]I. F. Schneider, A. E. Orel and A. Suzor-Weiner, Phys. Rev. Lett. 85 (2000) 3785.
[18]C. A. Nicolaides, Chem. Phys. Lett. 161 (1989) 547.